

Alzheimer's disease classification based on sparse functional connectivity and non-negative matrix factorization

Li Xuan¹ Lu Xuesong² Wang Haixian^{1,3}

(¹Key Laboratory of Child Development and Learning Science of Ministry of Education, Research Center for Learning Science, Southeast University, Nanjing 210096, China)

(²Department of Rehabilitation, Zhongda Hospital, Southeast University, Nanjing 210009, China)

(³School of Mathematics and Big Data, Foshan University, Foshan 528000, China)

Abstract: A novel framework is proposed to obtain physiologically meaningful features for Alzheimer's disease (AD) classification based on sparse functional connectivity and non-negative matrix factorization. Specifically, the non-negative adaptive sparse representation (NASR) method is applied to compute the sparse functional connectivity among brain regions based on functional magnetic resonance imaging (fMRI) data for feature extraction. Afterwards, the sparse non-negative matrix factorization (sNMF) method is adopted for dimensionality reduction to obtain low-dimensional features with straightforward physical meaning. The experimental results show that the proposed framework outperforms the competing frameworks in terms of classification accuracy, sensitivity and specificity. Furthermore, three sub-networks, including the default mode network, the basal ganglia-thalamus-limbic network and the temporal-insular network, are found to have notable differences between the AD patients and the healthy subjects. The proposed framework can effectively identify AD patients and has potentials for extending the understanding of the pathological changes of AD.

Key words: Alzheimer's disease; sparse representation; non-negative matrix factorization; functional connectivity

DOI: 10.3969/j.issn.1003-7985.2019.02.001

Alzheimer's disease (AD) is a neurodegenerative disease which is often found in the elderly group, characterized by symptoms including dementia and decline of cognitive function. A neuroimaging technique, resting state functional magnetic resonance imaging (rs-fMRI), provides a useful channel to study the pathological process of AD without requiring the patients to perform any tasks.

Received 2018-12-30, **Revised** 2019-03-28.

Biographies: Li Xuan (1990—), female, Ph. D. candidate; Wang Haixian (corresponding author), male, doctor, professor, hxwang@seu.edu.cn.

Foundation items: The Foundation of Hygiene and Health of Jiangsu Province (No. H2018042), the National Natural Science Foundation of China (No. 61773114), the Key Research and Development Plan (Industry Foresight and Common Key Technology) of Jiangsu Province (No. BE2017007-3).

Citation: Li Xuan, Lu Xuesong, Wang Haixian. Alzheimer's disease classification based on sparse functional connectivity and non-negative matrix factorization[J]. Journal of Southeast University (English Edition), 2019, 35(2): 147 – 152. DOI: 10.3969/j.issn.1003-7985.2019.02.001.

Designing classification frameworks for identifying AD patients on an individual basis is of great importance. However, it is a challenging task to extract discriminative information from the high-dimensional complex fMRI data.

Functional connectivity is a popular feature for AD detection. It is a commonly-used measurement for fMRI signals that depicts the temporal dependency of spatially distinct brain regions^[1]. Alterations in functional connectivity have been found in AD patients consistently by previous fMRI studies^[2-3]. One of the most widely-used methods to calculate functional connectivity is the Pearson correlation method. However, it only computes the association between a pair of nodes at one time, thus ignoring the possible influence from the other nodes. Besides, the resulting associations are typically dense and have negative values that are difficult to interpret.

Another important issue in AD detection is dimensionality reduction of the high-dimensional features. Generally, dimensionality reduction methods can be categorized into two groups: supervised methods and unsupervised methods. Supervised methods utilize the label information to obtain discriminative features. Nevertheless, in practice, the resulting features may vary from fold to fold when using the cross-validation procedure, thus making it tricky to interpret the results. In contrast, unsupervised methods do not require the label information, and consequently, they can be used as a preprocessing procedure on the whole dataset. Principle component analysis (PCA) is a widely-used unsupervised method for dimensionality reduction. However, the physical interpretation of the obtained components is not straightforward as PCA produces negative values. Recently, another matrix factorization approach, i. e., non-negative matrix factorization (NMF)^[4], has attracted growing attention in neuroimaging data processing. For example, the standard NMF method has been applied to extract features on positron emission tomography (PET) images for AD detection^[5]. The symmetric NMF method has been adopted to detect the community structure of brain functional networks on fMRI data in our previous work^[6]. NMF shows a distinct ability when performing dimensionality reduction and obtains interpretable components due to its non-negativity

constraint.

In this paper, we construct a novel classification framework for AD. Specifically, we adopt the non-negative adaptive sparse representation (NASR) method^[6-7], proposed in our previous work, to calculate the functional connectivity for feature extraction. In addition, we apply the sparse NMF (sNMF) method^[8] to conduct dimensionality reduction. NASR has achieved good performance in demonstrating functional connectivity. It computes the non-negative associations between one node and all the other nodes simultaneously. In the meantime, it adaptively enforces sparsity by taking the grouping feature of the highly-correlated fMRI signals into consideration. The sNMF method performs dimensionality reduction while improving the interpretation of the obtained components with the help of its sparsity constraint.

1 Proposed Classification Framework

1.1 NASR for feature extraction

Let $X = (\mathbf{x}_1, \mathbf{x}_2, \dots, \mathbf{x}_n) \in \mathbf{R}^{d \times n}$ be a matrix of the normalized fMRI time series of n nodes with d time points. NASR calculates the associations between \mathbf{x}_j and all the other nodes simultaneously by learning the coding vector $\mathbf{w}_j \in \mathbf{R}^n$. Mathematically, it is formulated as

$$\min_{\mathbf{w}_j \geq 0} \frac{1}{2} \|\mathbf{x}_j - X\mathbf{w}_j\|_2^2 + \lambda \|\mathbf{X} \text{Diag}(\mathbf{w}_j)\|_* \quad (1)$$

where parameter $\lambda > 0$ controls the sparsity level and $\text{Diag}(\mathbf{w}_j)$ is a diagonal matrix with \mathbf{w}_j as the diagonal. Each element $\mathbf{w}_{j,i}$ represents the association (i. e., functional connectivity) between node j and node i , and $\mathbf{w}_{j,j}$ is set to be zero. Differently from other sparse representation methods, NASR adopts a trace lasso norm $\|\mathbf{X} \text{Diag}(\mathbf{w}_j)\|_*$ as the regularizer, where $\|\cdot\|_*$ computes the sum of singular values. It adaptively trades off between l_1 -norm and l_2 -norm^[9]:

$$\|\mathbf{w}\|_2 \leq \|\mathbf{X} \text{Diag}(\mathbf{w})\|_* \leq \|\mathbf{w}\|_1 \quad (2)$$

which is useful for dealing with the highly-correlated fMRI data. Moreover, the non-negative constraint on \mathbf{w}_j enables only the samples that positively contribute to the representation to be preserved with a non-negative coefficient, further improving the interpretability of the associations. Finally, the symmetric association matrix is constructed by $\mathbf{G} = (\mathbf{W} + \mathbf{W}^T)/2$, where $\mathbf{W} = (\mathbf{w}_1, \dots, \mathbf{w}_n) \in \mathbf{R}^{n \times n}$. The optimization of NASR can be solved by using the alternating direction method to achieve a globally optimal solution^[7].

1.2 sNMF for dimensionality reduction

Given an association matrix $\mathbf{G} \in \mathbf{R}^{n \times n}$ of a subject, the upper triangle elements are transformed into a long feature vector $\mathbf{v} \in \mathbf{R}^f$, where $f = n(n-1)/2$. Then, the vectors of m subjects are stacked into a feature matrix $\mathbf{V} \in \mathbf{R}^{f \times m}$.

The sNMF method aims to represent \mathbf{v} in a low-dimensional space, by factorizing \mathbf{V} into a basis matrix $\mathbf{B} \in \mathbf{R}^{f \times k}$ and a coding matrix $\mathbf{H} \in \mathbf{R}^{k \times m}$ ($k \ll f$). In this way, each column of \mathbf{H} represents the feature vector of each subject with the reduced dimensionality k . The sNMF problem is formulated as^[8]

$$\min_{\mathbf{B}, \mathbf{H} \geq 0} \|\mathbf{V} - \mathbf{B}\mathbf{H}\|_F^2 + \beta \|\mathbf{B}\|_1 \text{ and } \max(\mathbf{B}_j) = 1 \quad (3)$$

$$j = 1, 2, \dots, k$$

where β determines the sparsity level of \mathbf{B} . The arbitrary scale of \mathbf{B} and \mathbf{H} is controlled by normalizing the maximum value of the column \mathbf{B} (i. e., \mathbf{B}_j) to be unity. The sNMF method learns a part-based representation due to its non-negativity. Furthermore, the sparsity constraint further improves the interpretability of the components \mathbf{B}_j .

According to Hoyer^[8], the optimization of \mathbf{H} and \mathbf{B} can be solved by using the multiplicative update rule and the projected gradient descent, respectively. Specifically, by fixing \mathbf{B} , \mathbf{H} is updated as

$$\mathbf{H} \leftarrow \mathbf{H} \cdot \frac{\mathbf{B}^T \mathbf{V}}{\mathbf{B}^T \mathbf{B} \mathbf{H} + \beta} \quad (4)$$

By holding \mathbf{H} fixed, \mathbf{B} is learned by using the projected gradient descent:

$$\mathbf{B} \leftarrow \mathbf{B} - \mu(\mathbf{B}\mathbf{H} - \mathbf{V})\mathbf{H}^T \quad (5)$$

where μ is the stepsize parameter. Then, all negative values in \mathbf{B} are set to be zero to ensure the non-negativity and the maximum value of each column is renormalized to unity.

1.3 Classification

The classification is performed by using the linear discriminant analysis (LDA) classifier with a leave-one-out cross-validation (LOOCV) procedure. The classification performance is evaluated in terms of accuracy (ACC), sensitivity (SEN) and specificity (SPE). The three measures are defined as $\text{ACC} = \frac{\text{TP} + \text{TN}}{\text{TP} + \text{FP} + \text{TN} + \text{FN}}$,

$\text{SEN} = \frac{\text{TP}}{\text{TP} + \text{FN}}$, and $\text{SPE} = \frac{\text{TN}}{\text{TN} + \text{FP}}$, where TP, TN, FP and FN refer to true positive, true negative, false positive and false negative, respectively. In addition, permutation tests (repeated for 1 000 times) are adopted to evaluate the statistical significance of the classification accuracy.

2 Experiment

2.1 Subjects and data

The rs-fMRI data of forty subjects with AD (age: 75.3 ± 7.1 years, 18 female) and forty-five normal controls (NC, age: 75.0 ± 5.5 years, 28 female) from the Alzheimer's Disease Neuroimaging Initiative (ADNI) dataset were used in this study. The subjects from the two groups were matched in age, sex and education level. All

subjects were scanned by using 3.0 T Philips scanners. The acquired rs-fMRI data for each subject consists of 140 volumes. Informed consent was obtained from all the individual participants included in the study.

2.2 Preprocessing

The rs-fMRI data were preprocessed following the widely-accepted pipelines by using the Data Processing Assistant for Resting-State fMRI (DPARSF) software^[10]. Specifically, the first 7 echoplanar imaging volumes were discarded. The remaining volumes of each subject were slice-timing corrected and realigned. The Friston-24 parameter model as well as the cerebrospinal fluid and white matter signals were regressed out. Afterwards, the signals were detrended and normalized to the Montreal Neurological Institute space by using the DART-EL procedure with T1 images. The following steps were to perform spatial smoothing with a 6 mm full width half maximum Gaussian kernel and bandpass filtering (0.01 to 0.08 Hz). All the subjects have an overall head motion of less than 2 mm or 2 degrees during scanning. Finally, the mean fMRI time series of 90 nodes, defined by the automated anatomical labeling template^[11], were extracted for each node.

2.3 Experimental settings

In the step of feature extraction, NASR is compared with the Pearson correlation for calculating the functional connectivity. The parameter λ of NASR is set to be 0.1, empirically for all subjects. The negative values of the associations derived by the Pearson correlation are flipped in the subsequent analysis. In the step of dimensionality reduction, sNMF is compared with PCA, with the number of components k (i.e., the reduced dimension) varying from 10 to 80 with a stepsize of 10. The parameter β of sNMF is set to be 0.01, and 20 runs with random initializations are repeated to select the best run in each computation. Therefore, four classification frameworks are evaluated in this experiment, which are NASR + sNMF, Corr (refers to the Pearson correlation) + sNMF, NASR + PCA, and Corr + PCA, respectively.

3 Results and Discussion

Fig. 1 shows the association matrices of one AD patient and one NC subject, derived by NASR and by the Pearson correlation separately. As can be seen, the association matrices derived by NASR achieve a remarkably higher sparsity than those derived by the Pearson correlation. NASR preserves only the most important non-negative associations among nodes, thus enhancing the interpretability and reducing the computational burden in the subsequent analysis.

Fig. 2 displays the low-dimensional components obtained by different frameworks with $k = 10$ (for PCA k refers

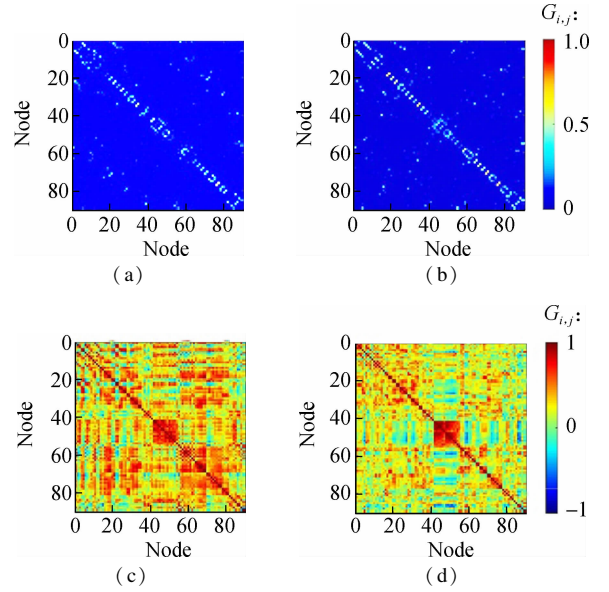


Fig. 1 Association matrices derived by NASR and the Pearson correlation. (a) AD patient by NASR; (b) NC subject by NASR; (c) AD patient by the Pearson correlation; (d) NC subject by the Pearson correlation

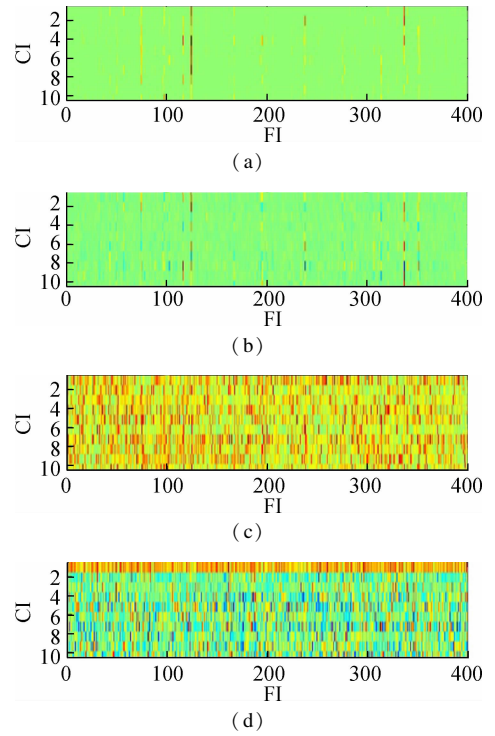


Fig. 2 Low-dimensional components derived by the four frameworks. (a) NASR + sNMF; (b) NASR + PCA; (c) Corr + sNMF; (d) Corr + PCA

to the first k components accounting for the largest variances), where CI refers to component index. For an easy comparison, 400 out of 4 005 features are randomly selected and displayed, where FI refers to the feature index. As can be seen, the components derived by sNMF have a higher sparsity than those derived by PCA. More

importantly, the components derived by sNMF have a more straightforward physiological interpretation, as sNMF groups functionally coherent nodes into one component due to its non-negativity. In other words, each component represents a brain sub-network with a specific function.

Fig. 3 shows the classification performance of the four frameworks under different values of k in terms of ACC, SEN and SPE. Overall, the proposed framework (i.e., NASR + sNMF) achieves the highest scores in all the three measures especially when k is small, while the Corr + PCA method achieves the lowest scores. The proposed framework attains the highest scores in ACC, SEN and SPE (0.812, 0.822 and 0.800, respectively) at $k = 30$, where the scores of the PCA-based frameworks fall below 0.7 with less than 80% of the variances explained. Therefore, a permutation test reveals that the classification accuracy of NASR + sNMF is statistically significant ($p < 0.001$).

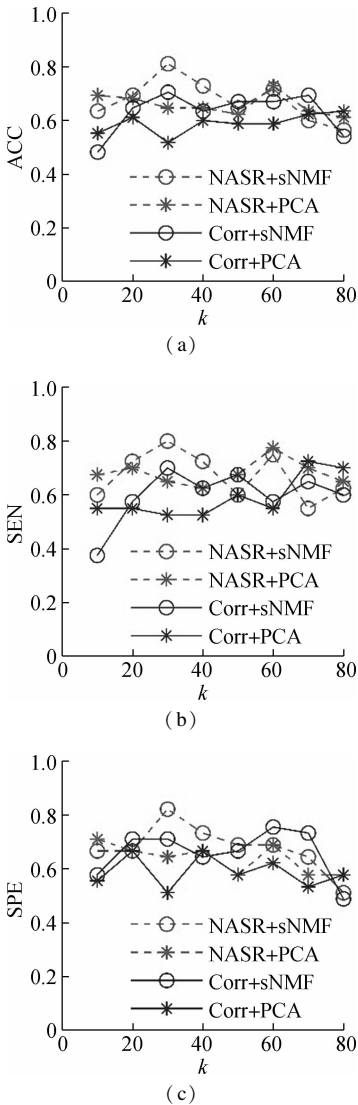


Fig. 3 Classification performance in terms of ACC, SEN and SPE of all the four frameworks. (a) ACC; (b) SEN; (c) SPE

Furthermore, we conducted rank-sum tests on the corresponding coefficients for each component derived by NASR + sNMF with $k = 30$ to find the sub-networks that carry the most discriminative information for classification. Among all the 30 components, one component (C1) shows a significant difference between the AD and NC groups ($p = 0.026$) and two components (C2 and C3) show a marginal significance ($p = 0.066$ and 0.079 , respectively), as shown in Fig. 4. The component C1, mainly covering the frontal, parietal and temporal lobes, refers to the default mode network (DMN). The component C2 mainly covers the basal ganglia, bilateral thalamus and limbic structures, while in C3 the temporal and insular areas play important roles. Evident alterations in these brain regions have been consistently discovered in AD patients by previous studies^[12-14].

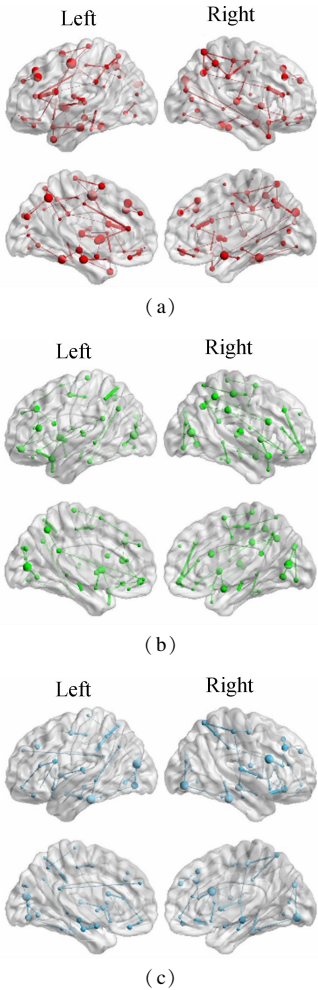


Fig. 4 Three discriminative components derived by NASR + sNMF with $k = 30$. (a) C1; (b) C2; (c) C3

To further validate the discriminative ability of the above three components, we performed classifications by using the coefficients of the three components (C1, C2 and C3) and their combination as features separately. The classification performance is shown in Fig. 5. It shows that all the three components achieve an accuracy

of above the chance level, where C2 achieves the highest accuracy of 0.588 (permutation test: $p < 0.05$). The combination of the three components substantially improves the accuracy to 0.659 (permutation test: $p < 0.001$). Besides, C1 and C2 achieve a high sensitivity of 0.825 and 0.875, respectively, while C3 achieves a high specificity of 0.800.

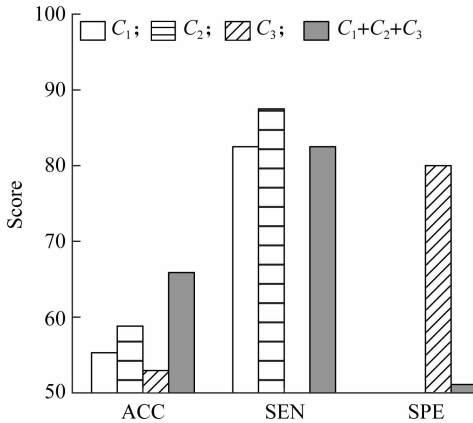


Fig. 5 Classification performance based on the coefficients of components C1, C2, C3 and their combination derived by NASR + sNMF

Many studies have designed classification frameworks for AD and achieved good performance^[15-17]. In this work, the proposed framework of NASR with sNMF aims at not only a good classification performance but also a physiologically meaningful interpretation. The proposed framework achieves a classification accuracy of above 80%, demonstrating its effectiveness in AD detection. Moreover, the derived components have a straightforward interpretation that each component represents a brain sub-network consisting of functionally coherent nodes. In the future work, the classification accuracy of the framework can be further improved by adopting more advanced classification algorithms and by combining other features.

4 Conclusions

1) We propose a novel classification framework for AD by applying NASR for feature extraction with sNMF for dimensionality reduction.

2) The proposed framework can effectively identify AD patients by achieving an accuracy, sensitivity and specificity of above 80%, which outperforms the competing frameworks.

3) It reveals three brain functional sub-networks that show notable discriminative information for AD detection, including the DMN, the basal ganglia-thalamus-limbic network and the temporal-insular network.

References

[1] Biswal B, Zerrin Yetkin F, Haughton V M, et al. Functional connectivity in the motor cortex of resting human

brain using echoplanar MRI [J]. *Magnetic Resonance in Medicine*, 1995, **34** (4): 537 – 541. DOI: 10.1002/mrm.1910340409.

[2] Balthazar M L F, Pereira F R S, Lopes T M, et al. Neuropsychiatric symptoms in Alzheimer's disease are related to functional connectivity alterations in the salience network[J]. *Human Brain Mapping*, 2014, **35**(4): 1237 – 1246. DOI:10.1002/hbm.22248.

[3] Teipel S, Drzezga A, Grothe M J, et al. Multimodal imaging in Alzheimer's disease: Validity and usefulness for early detection [J]. *The Lancet Neurology*, 2015, **14** (10): 1037 – 1053. DOI: 10.1016/s1474-4422 (15) 00093-9.

[4] Lee D D, Seung H S. Learning the parts of objects by non-negative matrix factorization[J]. *Nature*, 1999, **401** (6755): 788 – 791. DOI:10.1038/44565.

[5] Padilla P, López M, Górriz J M, et al. NMF-SVM based CAD tool applied to functional brain images for the diagnosis of Alzheimer's disease [J]. *IEEE Transactions on Medical Imaging*, 2012, **31**(2): 207 – 216. DOI:10.1109/tmi.2011.2167628.

[6] Li X, Hu Z L, Wang H X. Overlapping community structure detection of brain functional network using non-negative matrix factorization [C]//*International Conference on Neural Information Processing*. Kyoto, Japan, 2016: 140 – 147. DOI:10.1007/978-3-319-46675-0_16.

[7] Li X, Wang H X. Identification of functional networks in resting state fMRI data using adaptive sparse representation and affinity propagation clustering [J]. *Frontiers in Neuroscience*, 2015, **9**: 383-1 – 383-16. DOI:10.3389/fnins.2015.00383.

[8] Hoyer P O. Non-negative sparse coding [C]//*Proceedings of the 12th IEEE Workshop on Neural Networks for Signal Processing*. Martigny, Switzerland, 2002: 557 – 565.

[9] Grave E, Obozinski G R, Bach F R. Trace lasso: A trace norm regularization for correlated designs [C]//*Advances in Neural Information Processing Systems*. Granada, Spain, 2011: 2187 – 2195.

[10] Yan C G, Zang Y F. DPARSF: A MATLAB toolbox for “pipeline” data analysis of resting-state fMRI [J]. *Frontiers in Systems Neuroscience*, 2010, **4**: 13-1 – 13-7. DOI:10.3389/fnsys.2010.00013.

[11] Tzourio-Mazoyer N, Landeau B, Papathanassiou D, et al. Automated anatomical labeling of activations in SPM using a macroscopic anatomical parcellation of the MNI MRI single-subject brain [J]. *Neuroimage*, 2002, **15** (1): 273 – 289. DOI:10.1006/nimg.2001.0978.

[12] Klaassens B L, van Gerven J M A, van der Grond J, et al. Diminished posterior precuneus connectivity with the default mode network differentiates normal aging from Alzheimer's disease [J]. *Frontiers in Aging Neuroscience*, 2017, **9**: 97. DOI:10.3389/fnagi.2017.00097.

[13] Aggleton J P, Pralus A, Nelson A J D, et al. Thalamic pathology and memory loss in early Alzheimer's disease: Moving the focus from the medial temporal lobe to Papez circuit [J]. *Brain*, 2016, **139**(7): 1877 – 1890. DOI: 10.1093/brain/aww083.

[14] Harrison T M, Burggren A C, Small G W, et al. Altered memory-related functional connectivity of the anterior and

posterior hippocampus in older adults at increased genetic risk for Alzheimer’s disease[J]. *Human Brain Mapping*, 2016, **37**(1): 366 – 380. DOI:10.1002/hbm.23036.

[15] Rathore S, Habes M, Iftikhar M A, et al. A review on neuroimaging-based classification studies and associated feature extraction methods for Alzheimer’s disease and its prodromal stages [J]. *Neuroimage*, 2017, **155**: 530 – 548. DOI:10.1016/j.neuroimage.2017.03.057.

[16] Bi X A, Jiang Q, Sun Q, et al. Analysis of alzheimer’s disease based on the random neural network cluster in fMRI[J]. *Frontiers in Neuroinformatics*, 2018, **12**: 60. DOI:10.3389/fninf.2018.00060.

[17] Lian C F, Liu M X, Zhang J, et al. Hierarchical fully convolutional network for joint atrophy localization and alzheimer’s disease diagnosis using structural MRI [J]. *IEEE Transactions on Pattern Analysis and Machine Intelligence*, 2018, **99**: 1 – 14. DOI: 10.1109/tpami.2018.2889096.

基于稀疏功能连接及非负矩阵分解的阿尔兹海默症分类方法

李璇¹ 陆雪松² 王海贤^{1,3}

(¹ 东南大学学习科学研究中心儿童发展与学习科学教育部重点实验室, 南京 210096)
(² 东南大学附属中大医院康复医学科, 南京 210009)
(³ 佛山科学技术学院数学与大数据学院, 佛山 528000)

摘要:为了获得更具神经生理学意义的分类特征,提出了基于稀疏功能连接及非负矩阵分解的阿尔兹海默症分类方法.该方法基于功能核磁共振信号,采用非负自适应稀疏表示法计算脑区间的稀疏功能连接,以提取分类特征.然后,采用稀疏非负矩阵分解法进行特征降维,以获得具有明确物理意义的低维特征.实验结果表明该方法的分类准确率、灵敏度和特异度均优于其他对比方法.此外,发现了默认模式网络、基底神经节-丘脑-边缘结构网络及颞叶-脑岛网络在阿尔兹海默症病人和健康被试间具有明显差异.此方法能够有效地对阿尔兹海默症进行识别,同时具有加深对该病症功能病变理解的潜力.

关键词:阿尔兹海默症;稀疏表示;非负矩阵分解;功能连接

中图分类号:R318